Sebastian Schmitt (Autor)

Experimental and Numerical Investigations of Two-Phase Flow with Non-Isothermal Boundary Conditions under Microgravity Conditions

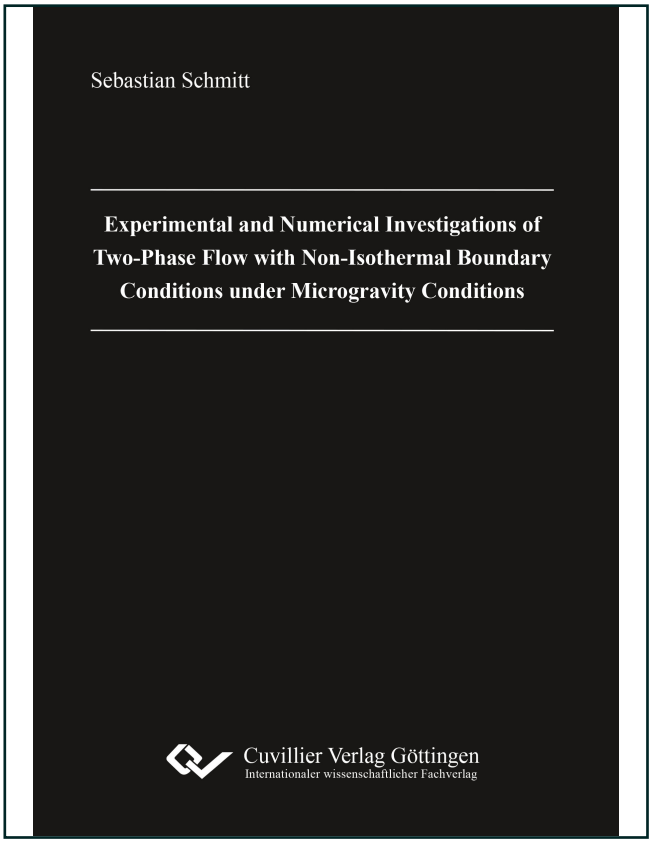

https://cuvillier.de/de/shop/publications/7485

Chapter 1

Introduction

1.1 Background

Currently, access to space requires a chemical propulsion system, that delivers the necessary thrust. This is realized by either solid or chemical propulsion (or a combination of both). The combination of liquid hydrogen (LH_2) as fuel with liquid oxygen (LOX) as oxidizer provides with 390 s the highest specific impulse[1] which results in a low propellant mass [27]. This combination has a long flight heritage on the first stage of Saturn V, Space Transportation System (STS) Shuttle [70] and Ariane 5, for example. For future concepts, such as the Space Launch System (SLS) [78] and the Ariane 6 Upper Liquid Propulsion Module (shown in Fig. 1.1), this efficient system requires further advancement.

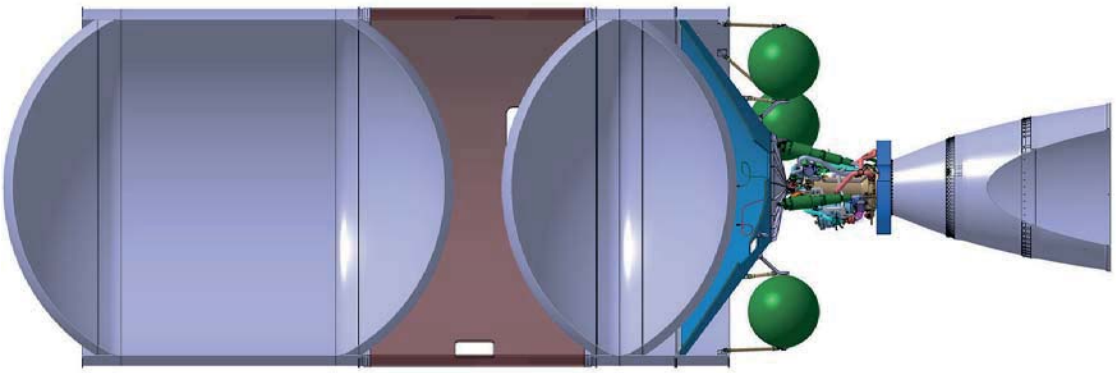

Figure 1.1: Preliminary Airbus DS A6 Upper Liquid Propulsion Module (ULPM), Courtesy of Airbus DS.

Cryogenic fluid management with varying accelerations becomes more important since new launcher concepts require a restartable cryogenic upper stage using liquid hydrogen/oxygen

[1] at $p = 7 \times 10^6$ Pa

for propulsion. A comprehensive understanding of the complex system of cryogenic fluids with a free surface within a closed tank with superheated walls is crucial to guarantee save operation. The accelerated phase ends with engine cutoff and the partially filled tanks enter the ballistic flight phase. At this instant of time hydrostatic forces caused by the acceleration vanish and the liquid-vapor interface changes from a flat surface to a shape with constant curvature. Throughout the reorientation process the free surface undergoes a damped axial sloshing motion.

Before the second engine burn a coasting phase may exist where the partially filled tank is exposed to weightlessness. Due to external heat loads (radiation, thermal conduction within the rocket structure) a thermal gradient builds up along the tank hull. Heat flux from the wall causes evaporation in the vicinity of the three phase contact line. The subcooled bulk outside the wall region leads to condensation along the free surface. These two mechanisms affect the pressure progression within the closed container. The shape of the free surface and its contact line have a major impact on the systems behavior.

1.2 Motivation

The here presented work addresses two main problems occurring in upper stage spacecraft propellant tanks.

First, the response of cryogenic fluids to a sudden change in gravity causes a reorientation of the liquid-vapor interface, also known as axial sloshing. This motion is influenced by thermal gradients along the tank wall. So far, no detailed study of this free surface motion of cryogenic parahydrogen with isothermal and non-isothermal boundary conditions has been conducted.

Second, phase change over the free surface has a major influence on the pressure progression in a tank, whereas the driving mechanisms strongly depend on the acceleration level. The integral influence of a present heat source in a normal gravity environment has been previously investigated by all means, but little information is available on the single mechanisms especially in weightlessness.

Obtained results from the executed work for this thesis help understanding how the free surface orientation is affected by external heat sources and how these heat fluxes influence phase change effects within the tank. Investigations were performed using numerical and experimental methods to supplement and validate the respective findings.

1.3 Outline

This thesis is divided into nine chapters. Following the background and motivation for this work, given in the introduction (Ch. 1), the theoretical background is introduced in Ch. 2. In this part the equations to solve basic and multiphase flow problems are specified together with the occurring physical phenomena, such as heat transfer and phase change. The used numerical tools are introduced and the characteristics of cryogenic liquids are briefly explained. An overview of the current state of the research regarding the experimental and numerical study of free surface reorientation, phase change effects and partially filled tanks with external heat loads under varying gravity conditions is given in Ch. 3.

In Ch. 4 all necessary equations and their boundary conditions, which are necessary to discuss single species, two phase flow problems with phase change, wall adhesion and conjugated heat transfer, are introduced. The set of equations is given for an infinitesimal small control volume in Cartesian and cylindrical coordinates addressing a compressible and an incompressible phase. The numerical implementation of the previously discussed set of equations within the used flow solvers is explained jointly with the solver theory in Ch. 5.

Chapter 6 describes the drop tower experiments and the setup of the numerical simulations. The experiment investigates a free surface in a party filled right circular cylinder upon a gravity step reduction. Along the tank wall, a well-defined temperature gradient could be imposed to investigate the influence of a superheated wall on the free surface reorientation. Two-dimensional (2D), axisymmetric simulations using the commercial flow solver Fluent v.15.0 were conducted to supplement the experimental findings. The simulations based on the suborbital flight experiment (SOURCE-II on MASER 12) are illustrated in Ch. 7. The purpose of this experiment was to investigate a single-species, two-phase fluid with a free surface and a superheated wall within 360 s of microgravity. This experiment was used to validate the numerical codes Flow-3D v.11.0.2 and Fluent v.15.0. Furthermore, the simulations provide substantial data to understand the driving mechanisms of the system. Main objectives were the pressure progression throughout several filling, pressurization and relaxation phases and the three phase contact line in presence of a superheated wall.

The results from the experiments and simulations introduced in the Chs. 6 and 7 are presented and discussed in Ch. 8. This chapter consists of two parts. First the topics concerning the free surface reorientation are addressed. In the second part the results from the numerical simulations of the SOURCE-II experiment are compared with the experimental data.

The final chapter (Ch. 9) firstly summarizes the results obtained from the experiments and simulations. In a second part, suggestions are made how to improve the experimental and numerical procedures and how to continue with research in this field.

Chapter 2

Theoretical Background

This chapter provides the theoretical background necessary for the understanding of this work. At first, the basic equations are introduced to describe fluid flow. In the following section, these equations are extended such, that they allow to enter a second phase. The third part lists methods of heat transfer in a given phase and between immiscible phases, followed by models to describe mass transfer between two phases of the same species. The last two sections give an overview of cryogenic liquids and how the previously introduced effects can be modeled in a numerical manner. The mathematical model and numerical implementation are of great importance for this work and are therefore discussed in detail in the Chs. 4 and 5.

2.1 Basic Equations

Most flow problems require the analysis of an arbitrary state of variable fluid motion defined by geometry, boundary conditions and the laws of mechanics. A control volume or large scale analysis is an accurate approach but is based on one dimensional properties on the boundaries. It is therefore useful for simple problems, like a straight pipe flow. For general observation of fluid flow, one must rely on differential or small scale analysis [89], which is introduced in Ch. 4. The more complex analysis results in a set of differential equations, which must be solved numerically, as shown in Ch. 5. The development of these equation can be found in numerous text books. This work is mostly based on [11, 28, 55, 89].

2.1.1 Reynolds Transport Theorem

For the analysis of a system, certain laws must be considered. First, there is the conservation of mass m over time t

$$\frac{\mathrm{d}m}{\mathrm{d}t} = 0\,. \tag{2.1}$$

Second, based on Newton's second law, the mass within a system starts to accelerate $\boldsymbol{a}$ if an external force $\boldsymbol{F}$ is acting, thus

$$\boldsymbol{F} = m\boldsymbol{a} = m\frac{\mathrm{d}\boldsymbol{v}}{\mathrm{d}t}\,. \tag{2.2}$$

Third, according to the first law of thermodynamics, any heat Q added to the system or work W done by the system changes the energy E of the system

$$\frac{\mathrm{d}Q}{\mathrm{d}t} - \frac{\mathrm{d}W}{\mathrm{d}t} = \frac{\mathrm{d}E}{\mathrm{d}t}\,. \tag{2.3}$$

Conversion of the basic laws 2.1 to 2.3 from a system analysis to a control volume (CV) analysis can be done with the Reynolds transport theorem, which is in the most general form

$$\frac{\mathrm{d}\phi_{sys}}{\mathrm{d}t} = \underbrace{\frac{\mathrm{d}}{\mathrm{d}t}\left(\int_{CV}\frac{\mathrm{d}\phi}{\mathrm{d}m}\rho\,\mathrm{d}V\right)}_{\text{change within the control volume}} + \underbrace{\int_{CS}\frac{\mathrm{d}\phi}{\mathrm{d}m}\rho\left(\boldsymbol{v}_{rel}\cdot\boldsymbol{n}\right)\mathrm{d}A}_{\text{flux terms}}\,. \tag{2.4}$$

It describes any fluid property (m, $m\boldsymbol{v}$ and E) of the system, represented by ϕ, with the change within the control volume and the flux across the surface. Since the control surface (CS) can move with $\boldsymbol{v}_{CS}$, one must define the relative velocity of the flow with respect to the moving CS, thus $\boldsymbol{v}_{rel} = \boldsymbol{v} - \boldsymbol{v}_{CS}$. The normal vector on the CS is $\boldsymbol{n}$.

2.1.2 Conservation Equations

Using the Reynolds transport theorem on eqs. 2.1 to 2.3 gives the conservation equations to characterize an arbitrary fluid flow problem. Mass conservation can be derived by using eq. 2.1 with eq. 2.4

$$\left(\frac{\mathrm{d}m}{\mathrm{d}t}\right)_{sys} = 0 = \frac{\mathrm{d}}{\mathrm{d}t}\left(\int_{CV}\rho\,\mathrm{d}V\right) + \int_{CS}\rho\left(\boldsymbol{v}_{rel}\cdot\boldsymbol{n}\right)\mathrm{d}A\,, \tag{2.5}$$

which defines the system's mass as the change of density over time within the CV and the mass entering or leaving over the CS. Replacing ϕ with the momentum $m\boldsymbol{v}$ gives the momentum conservation equation

$$\frac{\mathrm{d}}{\mathrm{d}t}\left(m\boldsymbol{v}\right)_{sys} = \sum\boldsymbol{F} = \frac{\mathrm{d}}{\mathrm{d}t}\left(\int_{CV}\boldsymbol{v}\rho\,\mathrm{d}V\right) + \int_{CS}\boldsymbol{v}\rho\left(\boldsymbol{v}_{rel}\cdot\boldsymbol{n}\right)\mathrm{d}A\,, \tag{2.6}$$

where all acting surface and body forces are represented by $\sum\boldsymbol{F}$. The energy conservation equation is derived with eq. 2.3 in eq. 2.4

$$\frac{\mathrm{d}Q}{\mathrm{d}t} - \frac{\mathrm{d}W}{\mathrm{d}t} = \left(\frac{\mathrm{d}E}{\mathrm{d}t}\right)_{sys} = \frac{\mathrm{d}}{\mathrm{d}t}\left(\int_{CV}e\rho\,\mathrm{d}V\right) + \int_{CS}e\rho\left(\boldsymbol{v}_{rel}\cdot\boldsymbol{n}\right)\mathrm{d}A\,, \tag{2.7}$$

with the intensive form of the energy $e = \frac{\mathrm{d}E}{\mathrm{d}m}$ which consists of the internal energy u, kinetic energy $\frac{1}{2}v^2$ and the potential energy gz

$$e = u + \frac{1}{2}v^2 + gz\,. \tag{2.8}$$

2.2 Multiphase Flow

The introduced equations can be used to analyze a single-phase flow problem. Once a second phase is present, such as liquid and its vapor, further equations are necessary. The conservation equations 2.5 to 2.7 must be solved for both phases. A set of equations must be developed to describe conditions at the newly formed boundary, the liquid-vapor interface. These boundary conditions will be discussed in detail in Sec. 4.5.2. In this work, the liquid-vapor interface or free surface is treated as a sharp interface with a sudden change between one phase to another. Observations of the liquid-vapor interface on a nanoscale level can be found in [15, 56]. The provided description of the free surface in presence or absence of gravity (see Sec. 2.2.3) are only valid for a right circular cylinder with an axisymmetric free surface. Changes of acceleration are considered to be abruptly, so without any transition phase.

2.2.1 Surface Tension

The liquid exposed to a second phase forms a free surface caused by the surface tension σ. Molecules at the surface are attracted to each other by van der Waals forces, so the free surface tends to minimize [15]. To increase the surface area, a certain amount of work is necessary, thus

$$\sigma = \frac{\mathrm{d}W}{\mathrm{d}A} = \frac{F\,\mathrm{d}s}{L\,\mathrm{d}s} = \frac{F}{L}\,. \tag{2.9}$$

The surface tension can also be expressed as the force applied along the free surface $\mathrm{d}s$ to increase the length L of the surface area. Temperature and pressure changes affect the surface tension. Increase in pressure or temperature results in a decreasing surface tension which converges to zero at the critical point [15].

A curved free surface causes a net pressure jump over the interface. Considering a bubble submerged in liquid, the curved interface has to be in equilibrium. The surface tension pulling on the free surface has to be balanced by a pressure difference $p^v - p^l$ between vapor (superscript v) and liquid (superscript l) [21, 56]. To compute the resulting force F_{res} we consider a point X on the free surface with the surface normal $\boldsymbol{n}$, depicted in Fig. 2.1. The normal $\boldsymbol{n}$ can be defined by two perpendicular planes. Both planes define a radius R_1 and R_2 with their origin

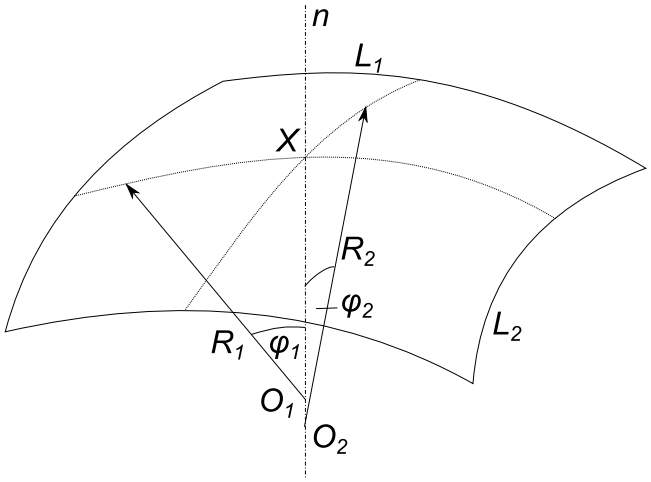

Figure 2.1: Part of a free surface with principal radii R_1 and R_2.

(O_1 and O_2) located along $\boldsymbol{n}$, which describe the curvature of the free surface. R_1 and R_2 are called principle radii. An arbitrary rectangular part of the interface $\mathrm{d}A$ has two sides L_1 and L_2 parallel to the previously defined planes. On both sides of $\mathrm{d}L_1$ tangential forces $F_1 = \sigma\,\mathrm{d}L_2$ are acting and analog for both sides of $F_2 = \sigma\,\mathrm{d}L_1$. Using the angles ϕ_1 and ϕ_2 one can write for the resulting forces normal to the surfaces:

$$F_{res,1} = 2F_1 \sin\phi_1\,, \tag{2.10}$$

$$F_{res,2} = 2F_2 \sin\phi_2\,. \tag{2.11}$$

For small angles, $\phi \ll 1$, one can write $\sin\phi \approx \phi$ and $\dfrac{1}{2}\,\mathrm{d}L = \phi R$, thus

$$\phi_1 = \frac{\mathrm{d}L_1}{2R_1}, \qquad \phi_2 = \frac{\mathrm{d}L_2}{2R_2}\,, \tag{2.12}$$

with eq. 2.12 in eqs. 2.10 and 2.11 gives

$$F_{res,1} = \sigma\frac{\mathrm{d}L_1\,\mathrm{d}L_2}{R_1}\,, \tag{2.13}$$

$$F_{res,2} = \sigma\frac{\mathrm{d}L_1\,\mathrm{d}L_2}{R_2}\,. \tag{2.14}$$

The resulting force $F_{res} = F_{res,1} + F_{res,2}$ is then

$$F_{res} = \sigma\left(\frac{1}{R_1} + \frac{1}{R_2}\right)\mathrm{d}L_1\,\mathrm{d}L_2\,. \tag{2.15}$$

Divided by the surface $\mathrm{d}A = \mathrm{d}L_1\,\mathrm{d}L_2$ gives the pressure jump

$$\Delta p = \sigma\left(\frac{1}{R_1} + \frac{1}{R_2}\right)\,. \tag{2.16}$$

Equation 2.16 is called the Young-Laplace equation. The higher pressure is always on the concave side of the surface.

2.2.2 Contact Angle

If the free surface is bounded by a third phase, like a wall (or immiscible fluid), a contact line (3D) or point (2D) can be found where the three phases (solid-liquid-vapor) meet. The angle between the solid-liquid interface (wall) and the tangent of the steady free surface at the contact point is called the static contact angle γ_s which evolves from the cohesion and adhesion forces [10]. The surface tensions of the three interfaces (solid-liquid, solid-vapor, liquid-vapor) must be in equilibrium [56],thus

$$\sigma^{s,l} + \sigma^{s,v} + \sigma = 0\,. \tag{2.17}$$

Young [92] performed a force balance tangential to the wall to derive the static contact angle from eq. 2.17.

$$\sigma \cos\gamma_s = \sigma^{s,v} - \sigma^{s,l} \tag{2.18}$$

For $0° < \gamma_s < 90°$ one speaks of wetting liquids and for $\gamma_s \geq 90°$ of non wetting liquids. Perfectly wetting liquids have a static contact angle of $\gamma_s = 0°$. Cryogenic liquids, such as liquid parahydrogen used for this work, have been identified to be perfectly wetting [52, 53, 73, 80, 84]. In general, the contact angle is not constant but changes with the contact line motion. An advancing contact line has a corresponding advancing contact angle and a receding contact angle for a receding contact line. The resulting hysteresis has been closely examined by Joanny and de Gennes [47] and de Gennes [20].

2.2.3 Stable Free Surface Under Varying Gravity Conditions

Concus [18] showed that a stable free surface shape is mainly influenced by gravitational acceleration g and surface tension σ, and is scaled with the Bond number

$$\mathrm{Bo} = \frac{\rho g L^2}{\sigma}\,. \tag{2.19}$$

The Bond number compares the hydrostatic pressure with the capillary pressure. For a cylindrical container with a circular free surface the tank radius R is used for the characteristic length L. For high Bond numbers ($\mathrm{Bo} \gg 1$) gravity is the dominating force which results in a flat surface as shown in Fig. 2.2 a). The free surface meets the wall under a certain static contact angle γ_s depending on the surface energies. At a certain length scale L_c, where $\mathrm{Bo} = 1$, hydrodynamic and capillary pressure are in equilibrium, thus

$$L_c = \left(\frac{\sigma}{\rho g}\right)^{1/2}\,. \tag{2.20}$$

The initial rise at a wall can be calculated with [55] as

$$z_{w,0} = L_c \left[2\left(1 - \sin\gamma_s\right)\right]^{1/2}\,. \tag{2.21}$$

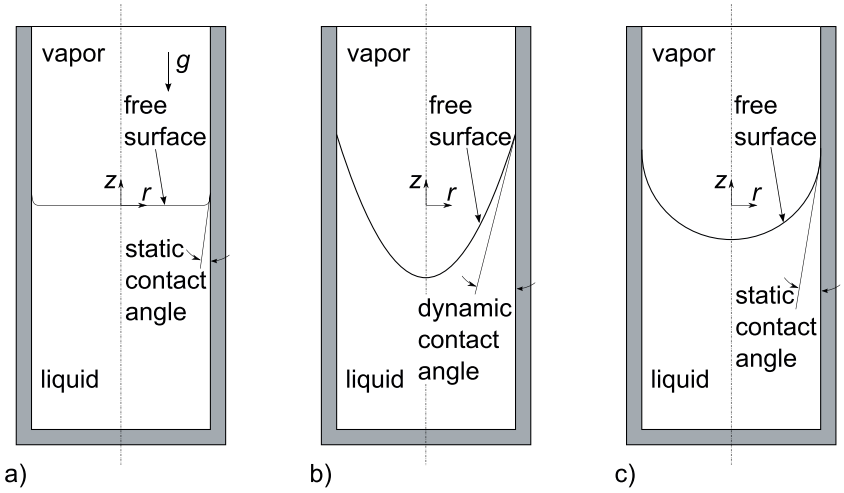

Figure 2.2: Free surface in a right circular cylinder a) in presence of gravity, b) throughout the dynamic reorientation process and c) under microgravity conditions.

Figure 2.2 b) shows the free surface in an unstable configuration throughout the reorientation process between normal gravity and microgravity. The stable free surface configuration in absence of gravity is presented in Fig. 2.2 c). In a microgravity environment low Bond numbers ($\mathrm{Bo} \ll 1$) are achieved and the influence of hydrostatic forces can be neglected. A free surface with constant curvature (circular segment) will be formed where the radius of the curvature is only dependent on the static contact angle [18].

2.2.4 Free surface reorientation

As explained in Sec. 2.2.3, the free surface curvature is dependent on hydrostatic and capillary forces. The former vanish in a microgravity environment and the liquid vapor interface reorientates from its flat shape to a configuration with constant curvature. This reorientation process can be divided into two time regimes [22, 65]. The sudden gravity step reduction causes a low pressure within the meniscus in the vicinity of the wall. The characteristic length to determine the characteristic time $t_{pu,Lc}$ and velocity $v_{pu,Lc}$ for this regime is the capillary length L_c from eq. 2.20. Together with the liquid density ρ^l and the surface tension σ one can determine the characteristic time as

$$t_{pu,Lc} = \left(\frac{\rho^l L_c^3}{\sigma}\right)^{1/2} = \left(\frac{\sigma}{\rho^l g_0^3}\right)^{1/4}, \tag{2.22}$$

where g_0 stands for the initial gravity. The characteristic velocity $v_{pu,Lc}$ results to

$$v_{pu,Lc} = \frac{L_c}{t_{pu,Lc}} = \left(\frac{g_0 \sigma}{\rho^l}\right)^{1/4}. \tag{2.23}$$

The first initial rise is followed by a second time regime that characterizes the global reorientation process with the cylinder radius R as the characteristic length. The characteristic time t_{pu} is then

$$t_{pu} = \left(\frac{\rho^l R^3}{\sigma} \right)^{1/2} . \tag{2.24}$$

and the corresponding velocity v_{pu}

$$v_{pu} = \frac{R}{t_{pu}} . \tag{2.25}$$

2.2.5 Damping

Michaelis [65] studied the damping of an axial oscillating (first mode) free surface in a right circular cylinder. Viscous dissipation occurs in the liquid motion but is also induced in the boundary layer along the container bottom and the wall. The moving contact wall induces further dissipative terms [39] which is important in the first time regime. The damping induced by the advancing contact line occurs due to the jump of single molecules at the contact line (Blake mechanism) and due to viscous hydrodynamic losses within the advancing liquid layer (de Gennes mechanism). For the second time regime Michaelis assumed a pinned contact line where only the first two mentioned mechanisms are of importance. The damping ratio induced by the waves (liquid motion) could be estimated as $D_{wa} \propto 2\,\mathrm{Oh}$. With the Ohnesorge number given as

$$\mathrm{Oh} = \left(\frac{\rho \nu^2}{\sigma R} \right)^{1/2} . \tag{2.26}$$

The more complex influence of the boundary layer was estimated with [65] under the assumption that the influence of the container bottom can be neglected

$$D_{bl} \propto \frac{2}{3} \left[\left(\left(\frac{1}{\cos \gamma_s} + \frac{1}{3} \right)^2 - 1 \right)^{1/2} - \tan \gamma_s \right] \mathrm{Oh}^{1/2} . \tag{2.27}$$

The damping coefficient caused by liquid motion D_{wa} and the one caused by the boundary layer D_{bl} can be summed up according to [16, 81], thus

$$D = C_{wa} D_{wa} + C_{bl} D_{bl} . \tag{2.28}$$

For small Ohnesorge numbers ,which is the case for this work, damping of the free surface motion is mostly caused by the influence of the boundary layer, since $D_{wa} \propto \mathrm{Oh}$ and $D_{wa} \propto \mathrm{Oh}^{1/2}$.

To avoid any influences from the container bottom, a sufficiently high fill level must be granted. Bauer and Eidel [9] investigated the influence of the bottom for a 90° contact angle. The container bottom has no effect for the first axial sloshing mode, if the ratio of the fill level to the cylinder radius exceeds 0.5.

2.3 Heat Transfer

Until now, only isothermal flows were considered and the temperature T did not play an active role. Introducing the temperature as a variable requires an equation to describe the relationship to the other variables. For compressible fluids the relation of temperature, pressure and density can be described with the ideal gas equation [5]

$$pV = m\Re T\,, \tag{2.29}$$

with $\Re$ as the specific gas constant. Using this assumption, one can calculate the change of the specific internal energy with the specific heat capacity at a constant volume as

$$u = \int_{T_0}^{T_1} c_v \,\mathrm{d}T\,. \tag{2.30}$$

Heat can be transferred by conduction, convection or radiation [5, 6, 11].

2.3.1 Conduction

Heat conduction is the flow of heat $\dot{Q}$ through a solid or fluid continuum. The driving gradient is the temperature gradient ∇T, whereby heat flows from areas of higher temperature to regions with lower temperature. The heat flow is further characterized by the thermal conductivity λ, a material property, which is dependent on temperature and pressure. Fourier's law describes this relation for the heat flux $\widehat{\boldsymbol{q}}$

$$\widehat{\boldsymbol{q}} = -\lambda \nabla T\,. \tag{2.31}$$

2.3.2 Convection

In a moving fluid heat is not only transferred by conduction but also by the macroscopic motion of the fluid. This mechanism, called convective heat transport, includes heat conduction and energy transport by the moving fluid. Newton's law of cooling describes the heat transfer over a solid-fluid interface with the solid temperature at the wall $T^s|_w$ and the far field fluid temperature T^f_∞. Besides the temperature difference the heat transfer coefficient α is required, which is usually unknown.

$$\widehat{q} = \alpha \left(T^s|_w - T^f_\infty \right) \tag{2.32}$$

2.3.3 Radiation

Any entity exchanges energy transmitted by electromagnetic waves to and from its environment. The maximum amount of heat flux is limited by its absolute temperature T, the temperature

of the environment T_∞ and the Stefan-Boltzmann constant $\overline{\sigma}$. The surface of the object and its condition can decrease the heat flux. This fact is represented by the emissivity ϵ, which is $\epsilon = 1$ for a black body.

$$\widehat{q} = \epsilon\overline{\sigma}\left(T^4 - T_\infty^4\right) \tag{2.33}$$

2.4 Phase Change

Phase change describes the transition of molecules from one phase to another, like melting/solidification, nucleate boiling and evaporation/condensation at the free surface. For this work only the latter one is of importance and therefore discussed. Basically one can say, that if the temperature of the vapor T^v is below the saturation temperature T_{sat} condensation occurs. If it is above the saturation temperature, liquid at the surface will tend to evaporate. The saturation temperature is connected to the saturation pressure and can be described with the Clausius-Clapeyron equation [5]. Any two points (subscripts 1 and 2) on the saturation curve can be expressed by the latent heat of evaporation Δh and the specific gas constant $\Re$ of the substance with

$$\ln\frac{p_1}{p_2} = \frac{\Delta h}{\Re}\left(\frac{1}{T_2} - \frac{1}{T_1}\right). \tag{2.34}$$

Phase change along the free surface can either exist within the micro-region, which is close to a solid wall on a micrometer scale [82, 83], or away from any solid [15, 57]. Both regions must be treated differently. The micro-region model describes the evaporation process caused by a heat flow from the hot wall to the liquid. It can be used for an accurate prediction of the contact angle in dependence of a given wall superheat or heat flux.

At a free surface in equilibrium and without radiative heat transport, the phase change can be described by the temperature gradients in the liquid and vapor in the vicinity of the free surface [15] with

$$\lambda^v\left(\frac{\partial T^v}{\partial n}\right)\bigg|_{if} - \lambda^l\left(\frac{\partial T^l}{\partial n}\right)\bigg|_{if} = \rho^l\left(v_n^l - \frac{\mathrm{d}z_{if}}{\mathrm{d}t}\right)\Delta h\,, \tag{2.35}$$

where $\dfrac{\mathrm{d}z_{if}}{\mathrm{d}t}$ describes the moving free surface in normal direction to compensate the mass flow across the interface. In nature and for numerical computations, the temperature gradients in the vicinity of the free surface can not be resolved properly. The Hertz-Knudsen equation, based on the kinetic theory of gases, is then usually used to calculate the net mass flux $\widehat{m}$

over a free surface with the molar mass M, universal gas constant $\overline{R}$ and the pressure and temperature on both sides of the interface

$$\widehat{m} = \frac{2\widetilde{\sigma}}{2-\widetilde{\sigma}} \left(\frac{M}{2\pi\overline{R}}\right)^{1/2} \left(\frac{p^v}{\sqrt{T^v}} - \frac{p^l}{\sqrt{T^l}}\right) . \tag{2.36}$$

This equation requires an accommodation coefficient $\widetilde{\sigma}$ as a probability factor, which is limited by $\widetilde{\sigma} \leq 1$ [15].

2.5 Numerical Implementation

The previous section gave a short overview of the physical background necessary to solve the flow problems in this work. Besides solving the conservation equations, numerical tools must be capable of modeling two-phase flow problems, conjugated heat transfer with an existing solid structure and liquid-vapor phase change in a closed system. Numerous academic and commercial codes are existent at the present time. The two flow solvers Flow-3D v.11.0.2 by *Flow Science* and Fluent v.15.0 by *Ansys* could fulfill the requirements and were available for the here presented studies.

2.6 Cryogenic Liquids

There is no defined temperature below one can speak of a cryogenic temperature regime. Scott speaks of a cryogenic environment, when the temperature drops below 150 K [76], while Jousten defines the cryogenic regime below 120 K [48]. In general, cryogenic liquids are liquids, that do exist as gases at ambient conditions [76]. Examples are liquid nitrogen, neon, methane, argon, hydrogen, oxygen and helium. Cryogenic hydrogen and oxygen are used widely in rocketry, such as the first stage of Airane 5 or the Space Shuttle, due to its high specific impulse.

Liquid parahydrogen, condensed from hydrogen vapor, was used for the drop tower experiments presented in Ch. 6. For this special case, the change from ortho (parallel) to para (anti-parallel) spin of the hydrogen molecules must be considered [14]. This conversion changes the material properties and releases heat which can be hazardous for the experimental apparatus.

Chapter 3

State of Research

This chapter provides an overview of the current state of research concerning the following fields for storable and cryogenic liquids:

- Free surface reorientation
- Influence of the contact angle on the free surface and influences on the contact angle
- Liquid-vapor phase change effects
- Effects of closed system pressurization

Research in this field started in the 1960s with the investigation of propellant tanks in accelerated and ballistic flight phases [38]. Great effort was taken to understand the surface reorientation and settling upon a gravity step reduction. The focus of current research is to predict the self and active pressurization of cryogenic tanks in microgravity. New techniques allow to simulate the complex coupled system between external heat sources (conduction, radiation), liquid, its vapor and a non condensable gas, if present. As far as applicable, all of these topics were subdivided into theoretical, experimental or numerical based research and distinguished into isothermal or non-isothermal cases.

3.1 Experimental Investigations of the Free Surface

3.1.1 Isothermal Experiments

Drop tower experiments to investigate the liquid-vapor interface behavior in a cylinder and sphere where conducted by Siegert et al. [79]. The experiment time (microgravity) was 2.25 s. Ethyl alcohol, carbon tetrachloride and a water ethyl alcohol mixture were chosen to observe the settling time, thus the time needed by the free surface to form a new stable shape. The